# GROWTH EFFECT OF CRYSTALLITES IN FE$_{82}$SI$_8$B$_{10}$ AMORPHOUS RIBBON

**A. Said Sikder[1], S. D. Nath[*1], M.N. I. Khan[2] and S. S. Sikder[1]**

[1]*Department of Physics, Khulna University of Engineering & Technology, Khulna-9203, Bangladesh*
[2]*Materials Science Division, Bangladesh Atomic Energy Centre, Dhaka - 1000, Bangladesh*

## ABSTRACT

*Fe$_{82}$Si$_8$B$_{10}$ amorphous ribbon which containing 82% of Fe and 18% of B and Si were prepared using rapid solidification technique. The samples were constantly annealed for 1 hour in the temperature range of 350°C-600°C. X-ray diffraction analysis (XRD) displays a large peak which is the diffusion hallow suggesting the amorphousity in its origin and formation of crystalline phase with the increment of annealing temperature at 450$^o$C. The magnetic ordering of the ribbon is determined as temperature functions by both AC and DC magnetization. At 450°C, the saturation magnetization (M$_s$) was found 143 emu/gm and with better value of real part of initial permeability at 450°C as well as better relative quality factor (RQF) was observed at the same temperature. The results are explained as due to higher heating rates than this Si diffuse in amorphous and lost the soft magnetic properties.*

*Keywords: Amorphous ribbon; XRD; VSM; Permeability; Relative Quality Factor.*

## 1. INTRODUCTION

Magnetic amorphous alloys have attracted great attention during several years, for both their fundamental physics of magnetism and technological levels (Zhou *et al*., 2020). During the fabrication of metallic glasses there may be some development of fault which reduces the performance of these soft magnetic metals. These annealing induced nano-crystallites distribute in amorphous matrix and have significant effect on magnetic properties. In addition, the phenomenon called "structural relaxation" also plays the important role in magnetic properties and annealing removes this relaxation stresses (Nabiałek *et al*., 2015; Sikder *et al*., 2020; Nabialek *et al*., 2014; Asgar *et al*., 1999). From structure aspects amorphous alloys are metastable nature renders them diverse thermodynamic behaviour upon heating at a temperature bellow onset crystallization and these structural changes metallic atom properties like thermal stability, plasticity, coercivity (Hc) crystallization and so on (Zhu *et al*., 2020). In magnetic glass, the macroscopic quantities which are the average kinetics of properties in the atomic scale are perturbed by structural disorder (Sikder *et al.,* 1999). It is well known that low temperature annealing will reduce the Hc as a result of the internal stress relief reducing magnetoelastic anisotropy and re orientation of the easy magnetization direction (Dai *et al*., 2017). Important thermodynamic parameter primary crystallization corresponds to the precipitation of an ordered bcc α-Fe(Si) solid solution embedded in an amorphous phase and secondary Fe2B phase for effect on the crystallization process (Sikder *et al*., 1999; Soltani *et al*., 2017; Öztürk *et al*., 2019). The Crystallites gran size and the percentage of Si content with heating temperature of such novel materials exhibits interesting properties including physical, chemical, magnetic and electrical properties compare to conventional coarse-grained counterparts. Consequently, the size and density of the nanocrystals and intergrain distances determine the soft magnetic properties of metallic alloys (Iqbal *et al.,* 2019; Calvin *et al*., 2003). The phase identification and gran size has been confirmed with the XRD experiment for both as as-cast and annealed samples to determine the crystallization onset temperature to evaluate the abridgment of annealing temperature. The magnetic measurement as known controlling annealing of amorphous metallic ribbons leads to excellent soft magnetic material and enhanced permeability and very low loss for important use of core materials. Ms and Hc determines of softness of a material. Annealing procedure, which suggests improvement of Ms and occurring of directional anisotropy by growing remanant (Mr) field, leads to magnetic hardening by increasing Hc are also destroyed of mechanical properties as ductility (Howlader *et al.,* 2017; Jiang *et al.,* 2017; Peixoto *et al*., 2018). The complex permeability in as quenched and annealed mantellic glass ribbon is discarded in terms of domain wall spinning as affected by the precipitation process and the initial permeability (μi) strongly affected by the presence of an electric due to its heating effect particularly in dynamic nature. The origin of the loss factor can be attributed to different domain effects leads to relative quantity factor (RQF) high value corresponding to a low loss factor including non-uniform and non-repetitive domain wall movements (Mondal *et al*., 2012; Zakaria *et al*., 1997).

## 2. MATERIALS AND METHODS

Crystallization kinetics study of $Fe_{82}Si_8B_{10}$ metallic amorphous ribbon on as-cast and annealed condition as well as to determine the optimum annealing temperature corresponding to $M_s$, $M_r$ and $H_c$ over which dynamic $\mu_i$ and RQF, cann be found and the sample can be used as a soft magnetic material, sample having composition $Fe_{82}Si_8B_{10}$, is processed in an arc furnace on a water-cooled copper base on an environment of pure $A_r$ at the core of Materials Research, National University of Hanoi, Vietnam. The purity of the constituent elements was, Fe (99.9%), Si (99.9%), and B (99.9%) and were obtained from Johnson Mathey (Alfa Aesar, UK). PHILIPS X′ Pert PRO X-ray diffractometer (Model no. PW3040, Phillips, Nevada, USA) have been used to study the crystalline phases of the samples with composition $Fe_{82}Si_8B_{10}$ in the Materials Science Division, Atomic Energy Centre, Dhaka-1000, Bangladesh. The specimens used were subjected to Cu-K$\alpha$ radiation with a primary beam of 40 kV and 30 mA with a phase size of 0.02º and Scan Phase Time 0.60 sec a 2θ scan was taken from 15.01º to 69.99º to establish potential simple peaks where Ni filter was used to minimize Cu-K$\alpha$ radiation. All study test results are evaluated using "X 'PERT HIGHSCORE" computer software. Crystallite size is determined using the Debye-Scherrer (Cullity, 1959) formula,

$$D_g = \frac{0.9\lambda}{\beta \cos \theta} \tag{1}$$

Crystalline nanograins, formed on the amorphous matrix of the ribbon in the process of heat treatment having the composition of Fe-Si, determined from the Pearson's relationship ((Pearson, 1958). The equation is

$$X = \left(\frac{a_0 - 2.8812}{0.0022}\right) \tag{2}$$

The magnetic activity of magnetic materials is measured by using a Vibrating Sample Magnetometer (VSM). A Quantum Design PPMS® DynaCool™ within an applied field of 20000 $O_e$ have been used to study the soft magnetic properties (DC properties) of the samples at the Materials Science Division, Atomic Energy Centre, Dhaka, Bangladesh. The frequency-dependent dynamic permeability (AC properties) of toroid formed specimens was calculated at room temperature using an impedance analyzer (Wayne Kerr 6500B, Wayne Kerr Electronics, West Sussex, UK). At first the Impedance Analyzer was calibrated using standard calibration kits. Then a section of ribbon was wound in the form of a toroid shape sample.

## 3. RESULTS AND DISCUSSIONS

### 3.1 X-ray Diffraction Analysis

X-ray Diffraction Technique (XRD) is used to evaluate the growth of crystallites with increment of annealing temperature. Annealing removes the stresses which could be formed during the fabrication of the amorphous ribbon. XRD Technique determines three kinds of structural parameter including lattice parameter, crystallite size and silicon content of amorphous α-Fe(Si) grains shown in figure 1 and table 1. It is very much well established that Fe-based amorphous and nanocrystalline ribbons shows diffraction pattern of α-Fe(Si) phase at (110) plane and $Fe_xB$ (x=1, 2, 3 …) on (200) plane in between 2 theta range of $40^o$ to $70^o$ (Zhi *et al.,* 1996; Liu *et al.,* 2013). The annealed $Fe_{82}Si_8B_{10}$ shows α-Fe(Si) phase peak on [110] plane and $Fe_2B$ phase peak on the [200] plane. The phase composition and peaks are being affected by the annealing processes. Figure 1 shows that when the specimens were annealed at 450°C it exhibited a small peak around 2θ=45° at the $d_{110}$ reflection spot and is generally referred to as a diffuse hallow. At this temperature, diffuse hallow suggests the sample's amorphous origin. It means at this temperature; there has been no detection of crystallization peak. Meanwhile, the broadened diffuse scattering diffraction peak of the sample is replaced by the shattered diffraction peaks and this indicates that the amorphous alloy is almost crystallized (Zhou *et al.,* 2020). At 450°C the shattered diffraction peaks indicates that the crystallization process started to a good extent. When the annealing temperature (Ta) reaches its first crystallization temperature, distinct crystalline diffraction peaks corresponding to the α-Fe phase can be observed on the XRD pattern, implying that the precipitation of the α-Fe phase from the amorphous matrix has occurred (Meng, 2021). As a result, the initial crystallization temperature is 450°C. When the annealing temperature is increased the diffraction peaks in the XRD diffraction pattern are shifted (Zhang, 2021) and the FWHM value gets smaller value with sharpening the peaks. When the sample was annealed at 520°C and °C the peak position has ben shifted. Also, for the higher annealing temperatures, sample shows that the FWHM value is getting smaller. This means that crystallization taking place to a greater degree at the higher annealing temperature. From the simple maximum of [110] reflections, the lattice parameter, the silicon content in bcc nanograins and crystallite size of α-Fe(Si) grain and FWHM can be calculated. All results are shown in table 1. The observation from figure 1 suggests that the samples annealed below the crystallization temperature keep their amorphous structure substantially. The phase Lattice parameter shown in Figure 2(a), was determined from Primary diffraction peak [α-Fe(Si)] using formula, $\alpha_o = d_{110}\sqrt{2}$ is gradually decreasing

due to the increase in the Si-content of the phase α-Fe(Si) due to the systematic yet marginal peak change to larger angles with increasing temperature happening because, pure Fe has the lattice parameter of 2.8664Å but in the present amorphous ribbon, the lattice parameter at various annealing temperature are significantly less than that of pure Fe.
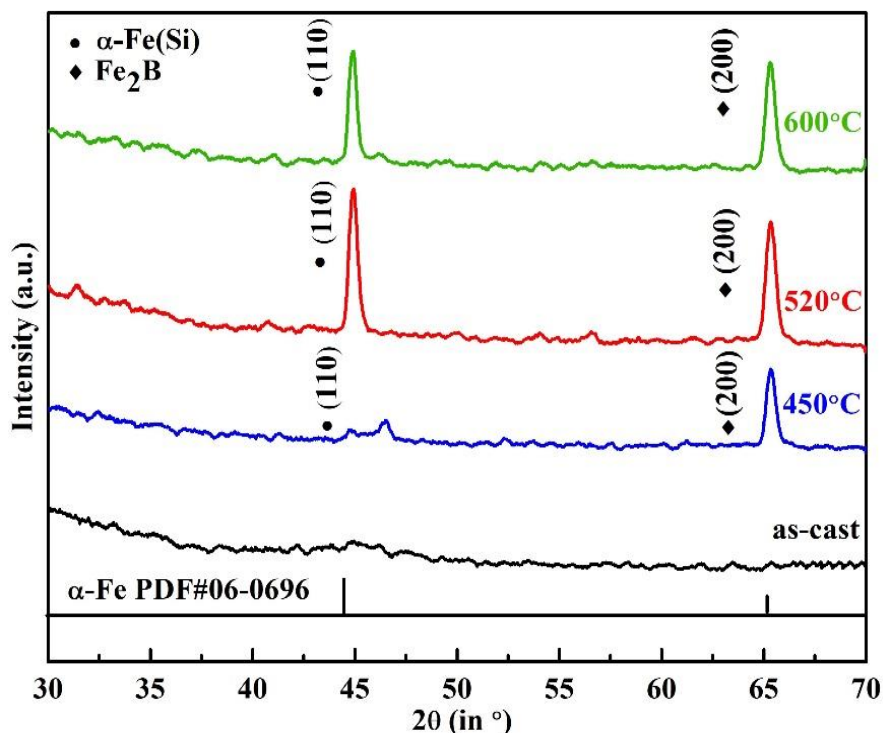


**Figure 1:** XRD spectrum of the amorphous ribbon $Fe_{82}Si_8B_{10}$ as cast and annealed at different temperatures at constant annealing time of 1 hour.

**Table 1:** XRD data of $Fe_{82}Si_8B_{10}$ in as-cast amorphous ribbon and different annealing temperatures at 1 hour annealing time.

| Annealing temperature in °C | Theta (deg) | $D^o$ (Å) | FWHM (deg) | $\alpha_o$ (Å) | $D_g$ (nm) | Si at (%) |
|---|---|---|---|---|---|---|
| As-cast | ------ | ------ | ------ | ------ | ------ | ------ |
| 450 | 23.262 | 1.9520 | 0.4723 | 2.7606 | 18 | 54.82 |
| 520 | 22.430 | 2.0205 | 0.2755 | 2.8574 | 31 | 10.82 |
| 600 | 22.406 | 2.0225 | 0.1181 | 2.8602 | 72 | 09.55 |

The diffusion phenomena in the α-Fe are occurring during the annealing because of the smaller atomic size of Si compared to Fe which is resulting in the contraction of Fe lattice. In the range of annealing temperature 450°C to 600°C, the crystallite size remains in the range of 18 to 72nm corresponding to soft magnetic $\alpha$-Fe(Si) phases. Above 520°C crystallites grows rapidly and attain maximum value 72nm at 600°C. Such facts show that the temperature of heat treatment should be limited in between 450 to 520°C in order to minimal grain size which is in between 18 and 31nm. The silicon contents of the alloy $Fe_{82}Si_8B_{10}$ at different annealing temperature 450, 520 and 600°C for constant one-hour annealing time are found to be in the range of 54.82 at % to 9.55 at % shown in Figure 2(b). All these results are presented in Table 1 and the pattern of annealing temperature change in the silicon content is shown in Figure 2(b).

The partitioned of the Si (%) in the amorphous α-Fe(Si) phase is maximum at 450°C. After 450°C, reduction of Si content has investigated up to 600°C. This is happening because of the diffusion of Si in nanograins due to the crystallization corresponding to formation of boride phase. Si has a smaller atomic size relative to Fe, it diffuses in the α-Fe(Si) lattice at various temperatures during annealing, which results in α-Fe lattice contraction. The more Si extends, the more the α-Fe lattice should be compressed and crystallite grows bigger. In addition, increasing the Si content results the reduction of the magnetic anisotropy and coercivity (Shokrollahi, 2009).
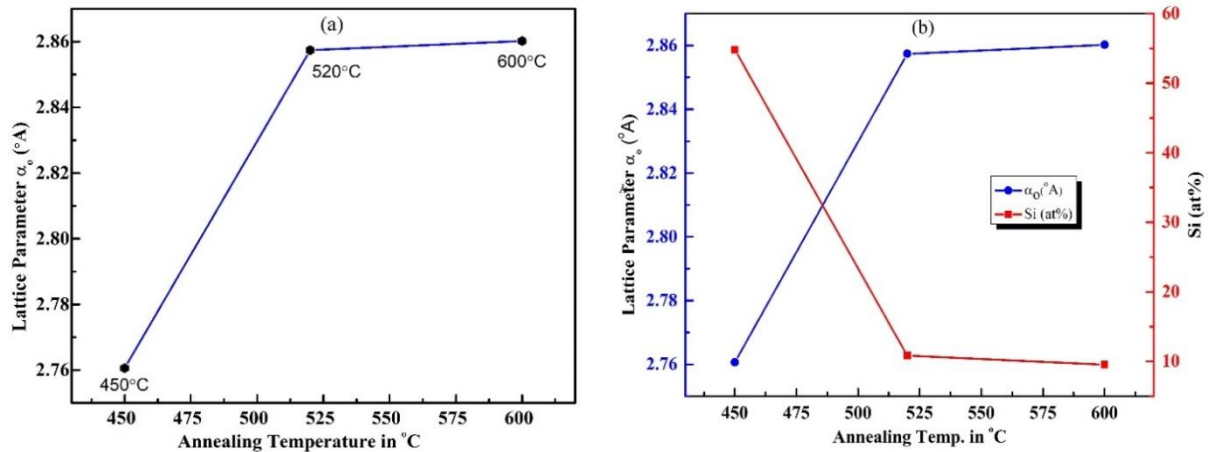
**Figure 2:** Effect of constant annealing (1 hour) on (a) lattice paremeter and (b) Si (%) of the sample.

### 3.2    Annealing Effects on DC Magnetic Properties

The magnetization measured as function of applied DC electric field is the DC magnetic properties of the soft magnetic materials. These include saturation magnetization ($M_S$), coercivity ($H_c$), remanant ($B_r$) magnetization and so on. $M_S$ of the annealed sample at room temperature has been measured and the annealing has been carried out for one-hour constant annealing time at 350 to 600°C which has been shown the figure 3 and are the magnetization process of the amorphous ribbons with different magnetic field. From these graphs it is distinctly seen that magnetization is saturated for all the materials in the annealed states inside a 20k $O_e$ application area. Recently, it is reported that the annealing temperature around 300°C for Fe-based amorphous alloys is not high enough to release all the bending stress of amorphous alloys, resulting in the increase of hysteresis loss (Azuma *et al.,* 2020). The observations from table 2 conclude that at as cast state the $M_S$ is 153emu/g which is the highest value also when it annealed at 350°C the $M_S$ has dropped to 95emu/g but with the increasing of annealing temperature this $M_S$ again increases. When the annealing temperature is 450°C the $M_S$ value is 143 emu/g. At this temperature the crystallite size is 18nm and which governs the soft magnetic properties (DC) as well as coercivity is as low as 29.25 which is lowest. This phenomenon simply concludes that this amorphous ribbon will show the optimum DC magnetic properties when this will be annealed at 450°C and will be very much dynamic in various magnetic devices like magnetic choke, magnetic springs, magnetic shields and so on. It is also observed from the table 2 that $M_S$ decreases at 520°C (126 emu/g) and again at 600°C it is increases (146 emu/g) which is quite close to it's as cast sate.
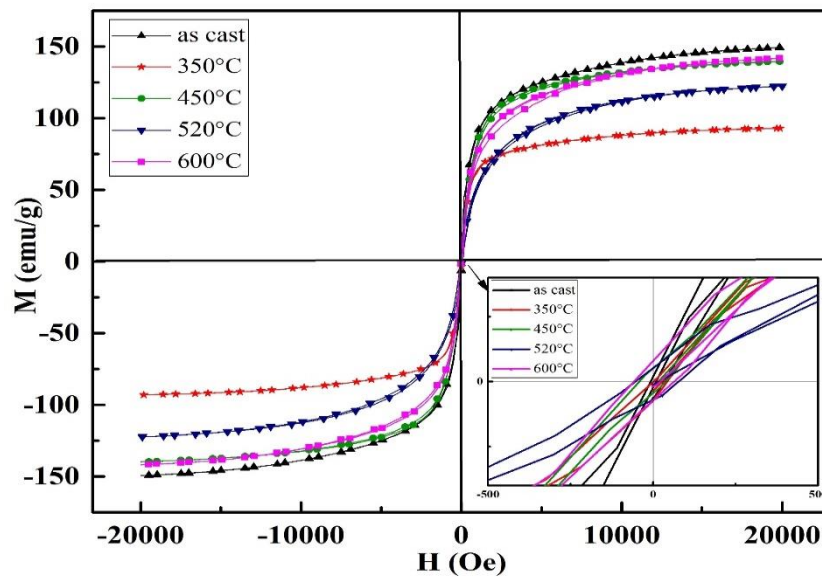


**Figure 3:** M-H loop of $Fe_{82}Si_8B_{10}$ amorphous ribbon at different annealing temperature for 1 hour annealing time.

**Table 2:** Saturation magnetization of $Fe_{82}Si_8B_{10}$ amorphous ribbon at different annealing temperature at1 hour.

| Annealing temperature, in °C | Saturation Magnetization, $M_s$ in emu/g | Remanence Magnetization, $M_r$ in emu/g | Coercive force, $H_c$ in Oe |
|---|---|---|---|
| As Cast | 153 | 3.03 | 39.70 |
| 350 | 95 | 1.86 | 19.52 |
| 450 | 143 | 3.46 | 29.25 |
| 520 | 126 | 3.88 | 59.65 |
| 600 | 146 | 3.67 | 39.80 |

These phenomena can be interpreted with the domain theory of ferromagnetism. The strong ferromagnetic exchange coupling negatively influences the saturation magnetization is reduced and on the other hand, the unreacted boron inclusions exert a strong pinning effect on the movement displacement and hinder the movement of the magnetic domain wall (Taghvaei, 2018). When the sample was annealed at 600°C this partially removes the pinning centers of the domain wall and improving the magnetic softness of this amorphous ribbon. But exception has occurred at 520°C annealed state. The soft magnetic properties of the Fe-based nanocrystalline ribbons are related to various phenomena, such as element enrichment, crystallization, phase separation, free volume annihilation and residual stress (Meng, 2021). At the temperature 520°C the sample can't release stresses because of forming of the precipitation of ferromagnetic α-Fe(Si) phase of Fe-Si-B ribbon and decreases the saturation magnetization. Both $B_r$ and $H_c$ is comparatively lower although with the increasing of annealing temperature (600°C) which conclude that in spite of increasing annealing temperature the sample shows dynamic soft magnetic performance but as the coercivity is almost two times (39.80 at 600°C) which creates limitations of being applied as a soft magnetic material.

### 3.3    Effects on AC Magnetic Properties

The parameters measured as function of frequency dependent applied AC electric field is the AC magnetic properties of the soft magnetic materials. These parameters include real part of initial permeability (μ'), imaginary part of initial permeability (μ"), and RQF. Temperature dependency of the real component of the initial complex permeability of the as-cast and annealed sample (350°C to 600°C) for one hour of constant annealing period as seen in figure 4(a). The figure shows that the low frequency value of the μ' increases with the rise in the annealing temperature and reaches the maximum value at 350°C annealing temperature and this annealed sample is minimum coercive force about $19.52O_e$ shown in table 2.
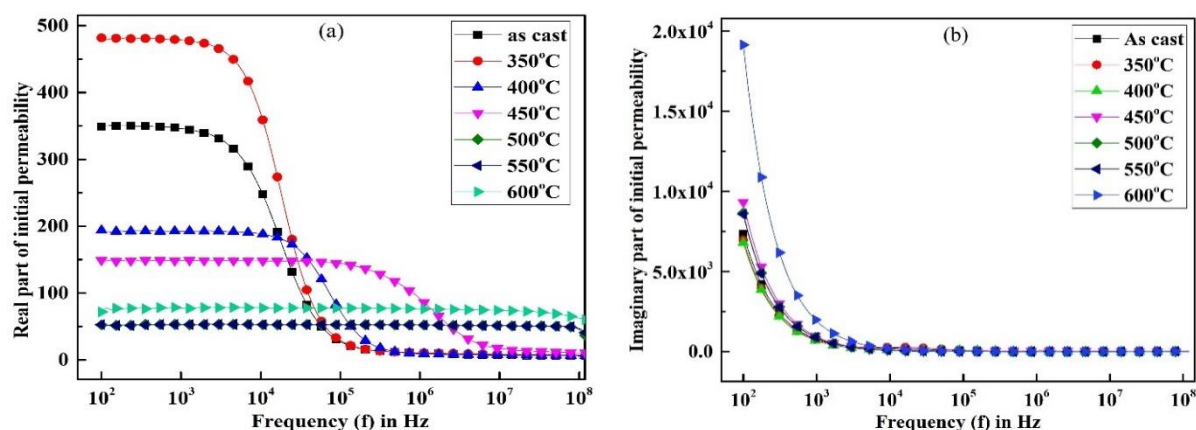


**Figure 4:** Frequency dependency of (a) real part and (b) imaginary part of initial permeability of $Fe_{82}Si_8B_{10}$ amorphous ribbon at 1 hour.

The maximum permeability μ'=483 value up to constant frequency range 10 kHz for the annealing temperature of 350°C compare as-cast ribbon μ' = 350 was observed due to the stress relaxation of the amorphous matrix i.e.; stress relief, increase of packing density of atom by annealing out of micro-voids changing the degree of chemical disorder. When the annealing temperature is higher than 400°C, initial permeability (μ') decrease rapidly. Drop in permeability in the annealing temperature 450°C can be due to the stress caused by rising crystallites in the amorphous matrix which concludes that this material can only be applicable in the low frequency range up to 10 kHz samples works as soft magnetic material with low loss. The results for the imaginary part of the initial permeability of samples are quite complimentary to the results shown in Figure 4(b).
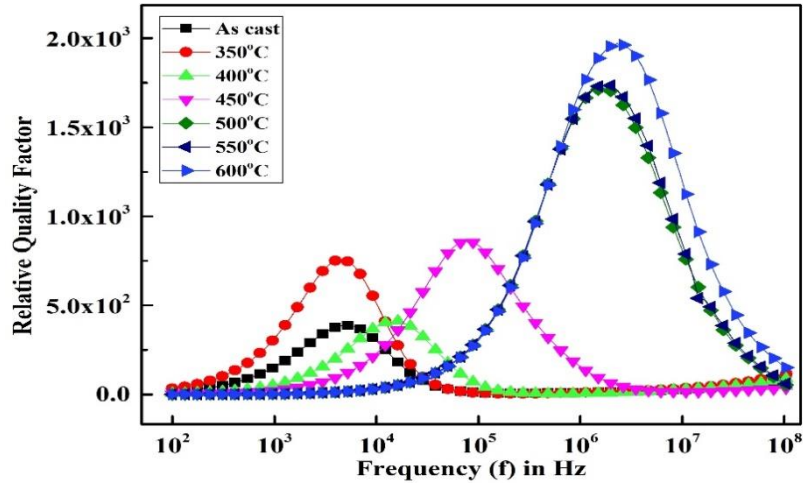
**Figure 5:** Frequency dependency of relative quality factor of $Fe_{82}Si_8B_{10}$ amorphous ribbon alloy for 1 hour.

Figure shows that the findings are quite similar to the results for the real part of the sample's dynamic permeability. The initial permeability for all low frequency samples is of relatively high value and corresponds to a high loss factor and a low-quality factor. The loss factor is given by the ratio of real and imaginary parts of the complex permeability i.e., $tan\delta = \frac{\mu'}{\mu''}$. The loss factor is caused by the eddy current loss as well as the spin reorientation process delay with regard to the external field. In general, the loss factor is found to be high for both low frequency and high frequency of the entire sample. The frequency dependence of RQF at constant annealing time one hour with different annealing temperatures is shown in Figure 5. It is observed from the Figure that the relative quality factor increases with the increase as-cast ribbon to annealing temperature ribbon and at 350°C display relative quality factor RQF of the order of 50 to 750. It is noticeable that higher value RQF=750 in the general operating soft magnetic behavior for amorphous matrix within the range 1 kHz to 110 kHz at annealed 350°C. For the sample annealed at 450°C, the highest quality factor value is found about order of 800 at $\mu' = 148$, which also indicates the best temperature for heat treatment to obtain the highest quality factor value for α-Fe(Si) phase grain size 18nm is minimum shown in Table 1. At high frequency in the range between 50 kHz to 1 MHz the quality factor for application area might be chosen.

## 4. CONCLUSIONS

The following conclusions can be drawn from the systematic study of the intrinsic and functional magnetic properties of crystallization:(i) The saturation magnetization (Ms) of as cast ribbon is 153 emu/g but when annealed at 350°C saturation magnetization (Ms) dropped to 95 emu/g with remanence magnetization, Mr = 1.86 emu/g and coercive force, Hc = 19.52 Oe and it also produce higher permeability value ($\mu'$=483) up to constant frequency range 10KHz holding the magnetically soft properties but when the annealing temperature was 450°C the non-crystallized sample shows saturation magnetization value, Ms=143 emu/g (near the value of as cast ribbon) with remanence magnetization, Mr=3.46 emu/g and coercive force, Hc=29.25 Oe as well as initial permeability value of $\mu'$= 148 up to constant operating frequency range 500KHz having minimum crystallite size 18nm. (ii) This gives a choice of optimum annealing temperatures 450°C, constant annealing temperature 1 hour, to attain the best soft magnetic properties with RQF value of 800. Annealing at this temperature the material can be used as a magnetic core material for the production of power transformer, magnetic storage devices, low frequency transformer (400Hz) etc.

### REFERENCES

Asgar, M.A., and Sikder S.S., 1999. Influence of glass forming material on atomic and magnetic ordering of Fe-based metallic glass. *Ind. J. Phy.*, *73*, 493-502.

Azuma, D., Ito N., and Ohta M., 2020. Recent progress in Fe-based amorphous and nanocrystalline soft magnetic materials. *J. of Magnetism and Magnetic Materials,* 501, 166373.

Calvin, S., Miller M. M., Goswami R., Cheng S. F., Mulvaney S. P., Whitman L. J., and Harris V. G., 2003. Determination of crystallite size in a magnetic nanocomposite using extended x-ray absorption fine structure. *Journal of applied physics*, 94(1), 778-783.

Cullity, B. D., 1959. Elements of X-Ray Diffraction. Addition Wesley, *London;262.*

Dai, J., Wang Y.G., Yang L., Xia G.T., Zeng Q.S., and Lou H.B., 2017. Structural aspects of magnetic softening in Fe-based metallic glass during annealing. *Scripta Materialia*, 127, 88-91.

Howlader, R. K., Shil S. K., Sikder S. S., and Saha D. K., 2017. Effect of annealing temperature on the complex permeability of $(Fe_{0.95}Co_{0.05})_{73.5}Cu_1Nb_3Si_{13.5}B_9$ nanocrystalline amorphous ribbon, *J. Mat. Sci.*, 5 (4), 144-148.

Iqbal, M.Z., Hossain M.A., Gafur M.A., Mahmud M.S., Saha D.K., and Sikder S.S., 2019. Effect of annealing on specific magnetization of Fe-Cr-Nb-Cu-Si-B with the partial replacement of Fe by chromium. *J. Phy. Commun.*, *3*(8), 085009.

Jiang, D., Zhou B., Jiang B., Ya B., and Zhang X., 2017. Study on soft magnetic properties of Finemet-type nanocrystalline alloys with Mo substituting for Nb. *physica status solidi (a)*, 214(10), 1700074.

Liu, Y., Yi Y., Shao W., and Shao Y., 2013. Microstructure and magnetic properties of soft magnetic powder cores of amorphous and nanocrystalline alloys. *J. magn. Magne. Mater.*, 330, 119-133.

Meng, Y., Pang S., Chang C., Bai X., and Zhang T., 2021. Nanocrystalline $Fe_{83}Si_4B_{10}P_2Cu_1$ ribbons with improved soft magnetic properties and bendability prepared via rapid annealing of the amorphous precursor. *J. of Magnetism and Magnetic Materials*, 523, 167583.

Mondal, S.P., Maria K.H., Sikder S.S., Choudhury S., Saha D.K., and Hakim M.A., 2012. Influence of annealing conditions on nanocrystalline and ultra-soft magnetic properties of $Fe_{75.5}Cu_1Nb_1Si_{13.5}B_9$ alloy. *J. Mat. Sci. Techn.*, 28(1), 21-26.

Nabiałek, M., 2015. Soft magnetic and microstructural investigation in Fe-based amorphous alloy. *J. alloys comp.*, 642, 98-103.

Nabialek, M.G., Pietrusiewicz P., Dospial M.J., Szota M., Błoch K., Gruszka K., Oźga K., and Garus S., 2014. Effect of manufacturing method on the magnetic properties and formation of structural defects in $Fe_{61}Co_{10}Y_8Zr_1B_{20}$ amorphous alloy. *J. Alloys Comp.*, 615, S51-S55.

Öztürk, S., İcin K., Gençtürk M., Göbülük M., Topal U., and Svec P., 2019. Surface and structural characterization of amorphous Fe, Co-based melt-spun ribbons subjected to heat treatment processes. *J. Non-Crys. Sol.*, 522, 119592.

Pearson, W. B., 1958. Lattice spacings and structures of metals and alloys. *Vols. I and II (Pergamon Press, Oxford, 1964, 1967).*

Peixoto, E.B., Mendonça E.C., Mercena S.G., Jesus A.C.B., Barbosa C.C.S., Meneses C.T., Duque J.G.S., and Silva R.A.G., 2018. Study of the dynamic of crystallization of an amorphous $Fe_{40}Ni_{40}P_{14}B_6$ ribbon through Johnson-Mehl-Avrami model. *J. alloys comp.*, 731, 1275-1279.

Shokrollahi, H., 2009. The magnetic and structural properties of the most important alloys of iron produced by mechanical alloying. *Materials & Design,* 30(9), 3374-3387.

Sikder, A. S., Nath S.D., and Sikder S.S., 2020. Influence of Annealing Temperature on the Crystallization Kinetics of $Fe_{82}Si_8B_{10}$ Amorphous Ribbon. *J. Eng. Sci.*, 11(1), 107-112.

Sikder, S.S., and Asgar M.A., 1999. The kinetics of atomic and magnetic ordering of Co-based amorphous ribbons as affected by iron substitution. *Thermochimica acta*, 326(1-2), 119-126.

Soltani, M.L., Touares A., Aboki T.A., and Gasser J.G., 2017. Thermal effect on structural and magnetic properties of $Fe_{78}B_{13}Si_9$ annealed amorphous ribbons. In *EPJ Web of Conferences*, 151, 07002.

Taghvaei, A. H., and Khoshrodi A. M., 2018. Characterization, thermodynamic analysis and magnetic investigation of new soft magnetic amorphous/nanocrystalline $Co_{50}Fe_{21}Ti_{19}Ta_5B_5$ powders produced by mechanical alloying. *Journal of Alloys and Compounds*, 742, 887-896.

Zakaria, A. K. M., Asgar M. A., Sikder S. S., and Ahmed F. U., 1997. The effect of annealing temperature on the complex permeability of Iron-Boron-Silicon amorphous ribbons, *Nuclear Sci. Appl.*, 6, 1 & 2, 47 - 57.

Zhang, B. H., Liu J. H., and Zhou H. T., 2021. Comprehensive study of the crystallization behavior, thermal stability, and magnetic properties of $Co_{66.5}Si_{15.5}B_{12}Fe_4Ni_2$ amorphous ribbon. *Journal of Non-Crystalline Solids,* 573, 121132.

Zhi, J., He K.Y., Cheng L.Z., and Fu Y.J., 1996. Influence of the element's Si/B on the structure and magnetic properties of nanocrystalline (Fe, Cu, Nb)$_{77.5}$Si$_x$B$_{22.5-x}$ alloys. *J. Magn. Magn. Mater.*, *153*(3), 315-319.

Zhou, X., Liu R., and Zhou H., 2020. A comprehensive study of microstructures and soft magnetic properties of amorphous $Co_{66}Fe_4Mo_2Si_{16}B_{12}$ tape wound core. *J. Magn. Magnet. Mat.*, *493*, 165729.

Zhu, L., Liu S.N., Lan S., Xu Y.M., Li C., Zheng H., Jiang S.S., Men J.R., Wang X.L., Pan F.M., and Wang Y.G., 2020. Structural Rearrangement at Medium-Range and its Effects on the Magnetic Properties and Crystallization Behaviors of a Fe-based Amorphous Alloy. J. Alloys Comp., 823, 53911.